1   **Mistaking plastic for zooplankton: risk assessment of plastic ingestion in the**

2   **Mediterranean sea**

3   [Fabri-Ruiz, S[1,2]., Baudena, A[1]]*., Moullec F[3]., Lombard, F.[1], Irisson, J.-O[1]., Pedrotti, M.L[1].

4   [1]Sorbonne Université, CNRS, Laboratoire d'Océanographie de Villefranche, Villefranche-sur-

5   Mer, France

6   [2] DECOD (Ecosystem Dynamics and Sustainability), IFREMER, INRAE, Institut Agro, Nantes,

7   France

8   [3]Department of Coastal Systems, Royal Netherlands Institute for Sea Research, P.O. Box 59,

9   1790 AB Den Burg, Texel, The Netherlands

10   Corresponding authors: alberto.baudena@gmail.com, salome.fabri.ruiz@ifremer.fr

11

12   *co-first authors

13   Abstract

14   Floating plastic debris is a pervasive pollutant in seas and oceans, affecting a wide range of

15   animals. In particular, microplastics (< 5 mm in size) increase the possibility that marine

16   species consume plastic and enter the food chain. The present study investigates this

17   potential mistake between plastic debris and zooplankton by calculating the plastic debris to

18   zooplankton ratio over the whole Mediterranean Sea. To this aim, in situ data from the Tara

19   Mediterranean Expedition are combined with environmental and Lagrangian diagnostics in a

20   machine learning approach to produce spatially-explicit maps of plastic debris and

zooplankton abundance. We then analyse the plastic to zooplankton ratio in regions with

high abundances of pelagic fish. Two of the major hotspots of pelagic fish, located in the

Gulf of Gabès and Cilician basin, were associated with high ratio values. Finally, we compare

the plastic to zooplankton ratio values in the Pelagos Sanctuary, an important hotspot for

marine mammals, with other Geographical Sub-Areas, and find that they were among the

larger of the Western Mediterranean Sea. Our results indicate a high potential risk of

contamination of marine fauna by plastic and advocate for novel integrated modelling

approaches which account for potential trophic transfer within the food chain.

I. Introduction

Plastic pollution is ubiquitous in the global ocean, from the sea surface to the seafloor

(Woodall et al. 2014, Esposito et al., 2022), and represents a major threat to socio-economic

services, tourism, and, ultimately, marine ecosystems (Aretoulaki et al., 2021; Beaumont et

al., 2019). It is estimated that 19 to 23 million metric tons of plastic waste entered the

aquatic systems in 2016, with an increasing trend expected in the next few years (Borrelle et

al., 2020; Lau et al., 2020). The Mediterranean Sea is among the world's seas most polluted

by plastic (Gerigny et al., 2019), with levels of concentration similar to those found in the

Great Pacific Garbage Patch (Cózar et al., 2015; Pedrotti et al., 2022). At the same time, this

quasi-enclosed sea is a key hotspot of marine biodiversity, with more than 17 000 species

recorded (Coll et al., 2010), and supports an overall fishery activity of ca. 9 billion dollars

every year (FAO 2020). Mediterranean marine ecosystems are, therefore, highly sensitive to

plastic pollution (Solomando et al., 2022; Soto-Navarro et al., 2021). Understanding the

magnitude of the impact of this pollutant on marine life is essential for conservation and

44   mitigation strategies (Galgani et al., 2014; Kershaw et al., 2019). In particular, it is

45   fundamental to evaluate the risk of plastic transfer along marine trophic webs, including

46   humans as well (Provencher et al., 2019; Rochman et al., 2015; Savoca et al., 2021). The

47   need to assess microplastic risk at the scale of the Mediterranean sea is important

48   considering the long distances crossed by mobile organisms (ie. cetaceans, fish, …). With the

49   increase of multiple anthropogenic pressures (including microplastics) on these species, the

50   risks must be evaluated at an appropriate spatial scale to mitigate their effect with adapted

51   conservation measures. However, this understanding is hampered by the scarcity of

52   available data, which usually cover only limited portions of the basin and differ in

53   methodology (e.g., Mansui et al., 2020). In addition, only few studies measured plastic and

54   organism concentrations concomitantly (Gérigny et al., 2022), making understanding of

55   plastic impact difficult. In addition, the role of circulation on the distribution of plastic and

56   zooplankton organisms is poorly unknown to date. An alternative method to estimate

57   plastic concentration is the use of Lagrangian models. These are based on the release of

58   virtual plastic particles which are then advected by current fields. From the virtual plastic

59   trajectories different information can be obtained, including zones of potential

60   accumulation or passage of plastic debris (Baudena et al., 2022, 2019; Beaumont et al.,

61   2019; Liubartseva et al., 2019; Mansui et al., 2020) dispersion. Only a few have, however,

62   been validated quantitatively with in situ data to date (Baudena et al., 2022). Furthermore,

63   Lagrangian models only simulate plastic dispersion, and usually do not include biological

64   activity such as the presence of zooplankton.

65   In the present study, we aim to quantify the relative presence of plastic compared to that of

66   zooplankton, to assess the potential mistake encountered by marine predators. For this

67　purpose, we used in situ observations from the Tara Mediterranean Expedition, which

68　constitutes the largest plastic dataset in the Mediterranean Sea to date: 122 stations

69　covering the entire basin with homogenised and standardised sampling techniques. We

70　considered plastic debris between 0.33—5.00 mm (usually referred to as *microplastics*).

71　Microplastics constituted an important proportion of the plastic debris at sea, and were the

72　vast bulk (~95%) of the debris collected during the Tara Mediterranean Expedition, making

73　plastic estimates more reliable (Pedrotti et al., 2022). Importantly, along with plastic debris,

74　zooplankton organisms of the same size class (0.33—5.00 mm) were concomitantly

75　sampled. We then combined them with a machine learning approach to study the

76　environmental drivers of plastic and zooplankton concentrations, unravelling some physical

77　processes responsible for their distribution. With this information, we obtained spatial

78　predictions for the whole Mediterranean Sea surface layer. These quantities were used to

79　estimate a ratio between plastic debris and zooplankton abundance. This value represents

80　the proportion of plastic debris with respect to the zooplankton organisms and can be seen

81　as an indicator of potential impact on marine life. A ratio of 0.1 means that, for every ten

82　zooplankton organisms present in a given seawater parcel, one plastic debris is present as

83　well. Previous studies only estimated this metric in correspondence with the location of the

84　sampling stations (Cole et al., 2011; Collignon et al., 2014; Doyle et al., 2011; Gérigny et al.,

85　2022; Gove et al., 2019 (plastic:larval Fish) ; Lattin et al., 2004; Moore et al., 2002; Pedrotti

86　et al., 2016). However, for conservation purposes, information on the impact of plastic at

87　larger spatial scales is needed: here, we provide an estimate over the entire Mediterranean

88　Sea of both plastic and zooplankton abundances as well as their ratio.

89　Furthermore, we use this metric to assess the overlap with potential predators through two

illustrative case studies. In the first, we only consider (i) species for which plastic ingestion has been reported (Fossi et al., 2014; Lefebvre et al., 2019; Pennino et al., 2020); (ii) species which are known to adopt non selective feeding strategies for certain prey sizes (Garrido et al., 2008, 2007; Queiros et al., 2019), as they could not be able to distinguish between plastic debris and zooplankton; (iii) species which are widely distributed over the entire Mediterranean basin (Bray et al., 2019); (iv) plastic debris and zooplankton in the same size class (0.33—5.00 mm) which can potentially confuse predators. As potential predators, we consider small pelagic fish (such as anchovies or sardines), which can acquire food through filter feeding behaviour. They feed on organisms smaller than 5 mm in size (Le Bourg et al., 2015) and have an important ecological and socio-economic role in the Mediterranean Sea. In the second case study, we focus on cetaceans by investigating the ratio values in the Pelagos sanctuary, which is a key foraging ground for marine mammals in the northwestern Mediterranean Sea (Croll et al., 2018; Fossi et al., 2014), and comparing them with Geographical Sub-Areas (GSAs) in the Mediterranean.

II.   Materials and Methods

We used a machine learning approach to correlate the response (i.e., in situ plastic and zooplankton abundances data obtained from the Tara Mediterranean Expedition) and explanatory (i.e., physical and biogeochemical data and Lagrangian and Eulerian diagnostics) variables. In the following sections, we described the data and the modelling framework used as well as the methodology employed to determine the plastic to zooplankton ratio, which is then applied to two case studies. To ensure reproducibility and transparency of results, we provided an ODMAP (Overview, Data, Model, Assessment and Prediction)

5

protein in the Supplementary Material. ODMAP is a standard protocol for species

distribution models based-approach that we used in our study (Fitzpatrick et al., 2021; Zurell

et al., 2020).

2.1. Response variables: in situ plastic and zooplankton data from Tara Mediterranean

Expedition

The Tara Mediterranean Expedition was conducted in the Mediterranean Sea between June

and November 2014. It sampled plastic debris and zooplankton in 122 stations across the

whole basin (Figure 1), representing the largest coupled plastic zooplankton database in the

Mediterranean Sea to date (Pedrotti et al., 2022). Plastic items were collected with a manta

net (height 25 cm, width 60 cm, mesh size 333 µm) towed at the sea surface and at an

average speed of ~2.5 knots for 60 minutes over a mean distance of ~4 km. Details of plastic

processing are described in Pedrotti et al., (2022), and are briefly reported here. Plastic

items were manually separated from zooplankton and organic tissue and scanned using the

ZooScan system (Gorsky et al., 2010) under dry conditions, while zooplankton organisms

were scanned separately under aqueous conditions. Particles and zooplankton were

automatically detected and their morphological attributes were extracted by post-

processing with Zooprocess and Plankton Identifier software. All obtained images were

imported within EcoTaxa (http://ecotaxa.obs-vlfr.fr, Picheral et al., 2017) and classified in

different taxonomic or particle categories. Microplastic (0.33—5 mm) abundances (in items

per square km; N/km^2) were calculated from particle counts. In addition, plastic debris

abundance was calculated also for the following size classes: debris between 0.33—1 mm;

debris between 1—5 mm; all plastic debris collected (i.e., larger than 0.33 mm). The size

137 class limits were chosen in order to test the robustness of the results. Similarly, total

138 zooplankton abundance per sample was calculated from zooscan and under the same size

139 classes defined for plastic debris abundance. Diel vertical migration was not observed over

140 the 24 hour day (Figure S1)

141
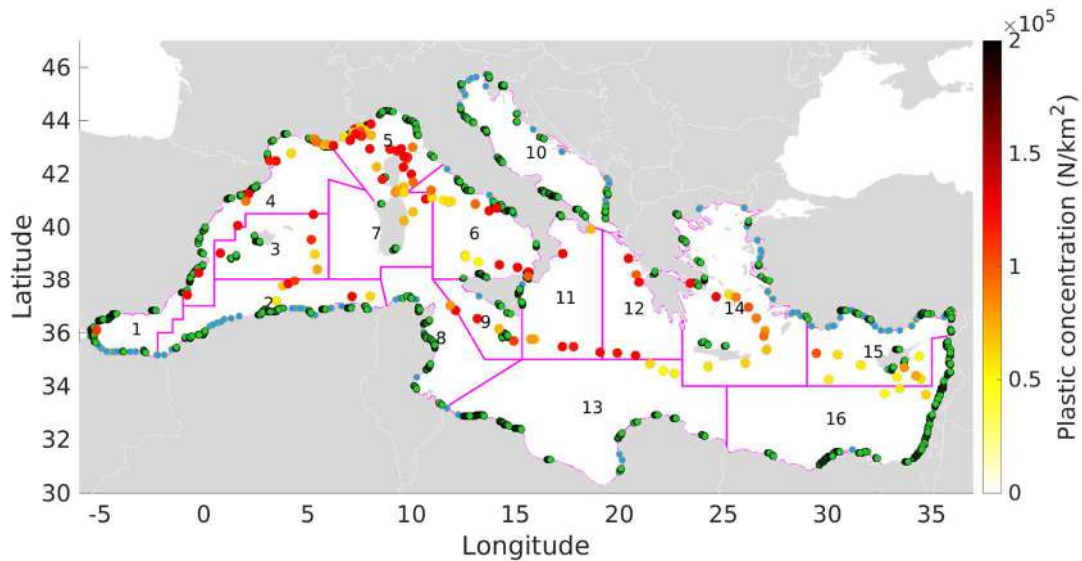
142 **Figure 1 : Overview of the domain studied**: Location of the 122 Tara Mediterranean

143 Expedition stations (colored circles) and corresponding estimated plastic concentrations

144 (right-hand yellow-to-red scale bar). Green and blue dots indicate the position of the coastal

145 cities and river mouths used as potential plastic sources. The purple dashed lines separate

146 the different Geographical Sub-Areas (GSAs) investigated in this study, indicated by a

147 number. 1: Alboran Sea, 2: Algeria, 3: Balearic Islands, 4: Northern Spain and Gulf of Lion, 5:

148 Pelagos sanctuary, 6: Tyrrhenian Sea, 7: Sardinia, 8: Tunisia, 9: Southern Sicily and Malta,

149 10: Adriatic Sea, 11: Western Ionian Sea, 12: Eastern Ionian Sea, 13: Southern Ionian Sea, 14:

150 Aegean Sea, 15: Northern Levant Sea and Cyprus, 16 : Southern and Eastern Levant Sea

151 **2.2. Explanatory variables**

2.2.1. Physical and biogeochemical data : salinity, temperature, nitrates, phosphates, dissolved oxygen concentration

Physical and biogeochemical data were extracted from the Copernicus Marine Environment Monitoring Service (CMEMS, http://marine.copernicus.eu, product MEDSEA_REANALYSIS_PHYS_006_004) at 1/16° resolution. The product was supplied by the Nucleus for European Modelling of the Ocean (NEMO), with a variational data assimilation scheme (OceanVAR) for temperature and salinity vertical profiles and satellite Sea Level Anomaly along track data. We only considered the surface layer (Simoncelli et al., 2014). Physical and biogeochemical data were provided at daily and weekly resolution, respectively. Climatologies were calculated by averaging over the six months of the Tara Mediterranean Expedition (June to November 2014; Table S1). Spatial resolution was decreased from 1/16° to 1/8° by bilinear interpolation to fit the same spatial resolution of the Lagrangian and Eulerian diagnostics. The environmental explanatory variables obtained include mean values for temperature, salinity, phosphate, nitrate and dissolved oxygen concentration.

Zooplankton concentration (mass content of zooplankton expressed as carbon in seawater, g/km^2; Seapodym model; Lehodey et al., 2010) provided by the GLOBAL_MULTIYEAR_BGC_001_033 product (CMEMS platform) was used to calculate a zooplankton climatology between June and November 2014 at 0.083° spatial resolution. The latter was used as a qualitative reference for the zooplankton projection (Subsec. 4.1), and not as an explanatory variable.

2.2.2. Lagrangian and Eulerian diagnostics

Velocity field and trajectory calculation: The velocity field was obtained by combining

175 together two hydrodynamical fields, both downloaded from the CMEMS platform. The first

176 product was the MEDSEA_REANALYSIS_PHYS_006_004, which provides surface currents and

177 includes the geostrophic and the Ekman components. It has a spatial resolution of 1/16° and

178 a temporal resolution of one day. The second product was the

179 MEDSEA_HINDCAST_WAV_006_012. It provides drift due to waves (Stokes drift). It has a

180 spatial resolution of 1/24° and a temporal resolution of one day. The velocity fields were

181 spatially and temporally interpolated (bilinear interpolation) and summed together,

182 providing the final velocity field (1/24°; 1 hour). Thus, the surface currents used take into

183 account the Stokes drift, which indirectly includes windage, an important component for

184 microplastic transport in marine environments (Onink et al., 2019), especially in the

185 Mediterranean Sea (Liubartseva et al., 2018). As zooplankton samplings were collected at

186 the same depth as plastic debris, we used the same velocity field for both explanatory

187 variables. Trajectories were calculated with a 4th order Runge-Kutta scheme in both space

188 and time, with a time step of 20 minutes.

189

190 **Lagrangian and Eulerian diagnostics description:** Different Lagrangian and Eulerian

191 diagnostics were used as explanatory variables. Lagrangian diagnostics were derived from

192 trajectories, whereas Eulerian diagnostics were obtained by properties at a fixed location.

193 The Eulerian diagnostics calculated were: *Absolute velocity*: $U=sqrt(u^2+v^2)$, with *u* and *v*

194 being the zonal and meridional component of the velocity field; *Kinetic Energy* = u^2+v^2

195 which, together with the absolute velocity is considered as a proxy of the intensity of the

196 currents; *Vorticity*: denotes the presence (when positive or negative) or absence (when

197 close to 0) of eddies; *Okubo-Weiss*: When negative (positive), this metric indicates a water

198 parcel inside (outside) an eddy; *Turbulent Kinetic Energy (TKE)*: This metric analyses the

199 standard deviation of the velocity field time series and quantifies whether a region was

200 subjected to strong turbulence. The Lagrangian diagnostics calculated were: *Finite-Time*

201 *Lyapunov Exponents (FTLE)*: FTLEs quantify the rate of separation due to currents. They are

202 used to identify barriers to transport or regions affected by strong turbulence (Baudena et

203 al., 2021; d'Ovidio et al., 2004); *Lagrangian Betweenness*: this metric is used to identify

204 regions that act as "bottlenecks" for the circulation, i.e. in which water parcels of multiple

205 origins pass and then go to several different destinations (Ser-Giacomi et al., 2021);

206 *Retention time*: this metric estimates the amount of time a water parcel spent inside an

207 eddy (if it was inside it) (d'Ovidio et al., 2015); *Lagrangian divergence*: this metric calculates

208 the Eulerian divergence along the backward trajectory. When negative (positive), it indicates

209 convergence (divergence) of water masses, and can be used as a proxy of downwelling

210 (upwelling) Hernández-Carrasco et al., (2018); *Lagrangian Plastic Pollution Index (LPPI)*: this

211 metric estimates the amount of plastic debris in a water parcel based on the plastic sources

212 (cities and rivers, blue and green dots in Fig. 1) encountered along the water parcel's

213 previous path. The water parcel "encounters" a plastic source when it passes below a

214 distance threshold from it (details in Pedrotti et al., 2022).

215 As for the physical and biogeochemical explanatory variables, climatologies of Lagrangian

216 and Eulerian diagnostics were calculated between June and November 2014 at 1/8° of

217 spatial resolution over the entire Mediterranean Sea. Details about the different parameters

218 used for each of the diagnostics are reported in Supplementary Table S2.

219 **2.3. Modelling framework: Xgboost models**

220 **2.3.1. Collinearity between explanatory variables**

221 Multicollinearity occurs when two or more explanatory variables in a multiple regression

222   model are highly correlated, which means that one can be predicted linearly from the

223   others with a high degree of accuracy. Multicollinearity can cause data redundancy in the

224   explanatory variables which can lead to model overfitting or reduction in model predictive

225   ability (Dormann et al., 2013). If multicollinearity patterns differ between fitted data in the

226   model and new data, large errors could be introduced in the predictions. To restrict these

227   possible biases, multicollinearity between explanatory variables was initially examined using

228   variance inflation (VIF) factors in a stepwise procedure (Dormann et al., 2013). VIF is

229   computed from equation [1], where R^2_j is obtained from a regression between variable j^{th}

230   against all other explanatory variables.

231

232 $$VIF_j = \frac{1}{1-R^2_j} \ [1]$$

233

234   In a stepwise procedure, the function calculates VIF values for all explanatory variables,

235   removes the variable with the highest value, and repeats until all VIF variable values are

236   below a given threshold (here 5). Finally, we computed Spearman pairwise correlation (r_S)

237   between descriptors and removed one of the two descriptors when correlation values of r_S

238   were above 0.7 (Dormann et al., 2013). Analyses were performed using the usdm (Babak,

239   2015) and corrplot (Wei et al., 2017) R packages. Table S3 lists the remaining variables used

240   in Xgboost models for each category.

241   **2.3.2. Parameterization and calibration of XGboost models**

242   The extreme gradient boosting (XGBoost) modelling approach (Chen and Guestrin, 2016)

243   was used to model plastic debris and zooplankton abundances for each size class. Xgboost is

244   an efficient gradient machine learning method that combines two algorithms: first, simple

245 and small regression trees, calculated on random subsets of data while minimising residuals;

246 and subsequently boosting, which combines all the models into a unique solution (for

247 statistical details see Chen and Guestrin, 2016). XGBoost models are able to fit complex

248 functions, which could reflect the complexity of processes shaping plastic debris and

249 zooplankton patterns. Xgboost models were performed using the xgboost R package (Chen

250 et al., 2015).

251 Cross validation procedure was used to estimate the best parameters of the xgboost model.

252 This procedure uses a single parameter k that refers to the number of groups for a given

253 dataset to be split into. In our case, we used k=4. For each group, we take the remaining

254 groups as a training data set and use the selected group to evaluate the model. This

255 procedure was performed for different xgboost parameters and poisson distribution:

256 number of trees (1 to 900), maximum depth (2, 4, 6) where the higher is the value the more

257 complex the model is, eta (0.005, 0.01, 0.02, 0.03, 0.04) which is the learning rate,

258 min_child_weigth (1, 5) which defines the minimum sum of weights of all observations

259 required in a child (used to control over-fitting). Best parameters were selected by

260 minimising the negative log-likelihood for Poisson regression. We evaluated the model using

261 the R^2 coefficient between observed and predicted data. Because several distance threshold

262 values were provided for plastic data (based on the LPPI), we fitted models for each and

263 kept the best one (Table S4).

264 **2.3.3. Prediction and projection**

265 The partial dependence plots (PDP) technique (Friedman, 2001) was used to achieve a

266 graphical representation of the marginal effect of a variable on the response variable. We

267 also extract variable importance from the model, which shows how a feature is important in

268 making a branch of a decision tree purer. A high percentage means important explanatory

269 variables which constrain response variables. Calculated functions in the model were then

270 used to extrapolate plastic debris and zooplankton abundances for each grid cell over the

271 entire Mediterranean Sea at a period corresponding to June-November 2014. We projected

272 mean plastic debris and zooplankton abundances and associated standard deviations.

273

274 **2.4. Plastic to zooplankton ratio definition**

275

276 Using zooplankton and plastic debris abundance projections over the entire Mediterranean

277 Sea, we calculated the plastic debris to zooplankton ratio (amount of plastic debris divided

278 by the amount of zooplankton) at 1/8° of spatial resolution. For each grid cell i, the ratio was

279 obtained by dividing the plastic and the zooplankton abundances (expressed in N/km^2) of

280 the same size class j:

$$Ratio_{i,j} = \frac{Plastic\ abundance_{i,j}}{Zooplankton\ abundance_{i,j}} \quad (1)$$

281

282 Equation 1 implies that, for example, if the ratio equals 0.1, for every 1000 zooplankton

283 organisms in a given water parcel 100 plastic debris of similar size is present. The ratio was

284 calculated using plastic debris and zooplankton organisms of size classes between 0.33—5

285 mm. Ratios calculated using different size classes (Subsec. 2.1) are reported in

286 Supplementary Materials. The uncertainty on the ratio was calculated with the variance

287 formula using the plastic and zooplankton associated standard deviations and Equation (1).

288 The ratio obtained using the size class of 0.33—5 mm was evaluated (i) in the Pelagos

289 Sanctuary, a hotspot for cetaceans, representing a foraging ground for different whale

290 species (Morgado et al., 2017). The ratio in the Pelagos Sanctuary was compared with the

291 ratio calculated in the Mediterranean GSAs (Fig. 1). GSAs were obtained from the FAO

292 platform (https://www.fao.org/gfcm/data/maps/gsas/en/). In order to have GSAs of similar

293 surface area, we merged together the following GSAs: Northern Alboran Sea, Southern

294 Alboran Sea, and Alboran Island, creating the Alboran Sea GSA (GSA 1); Northern Spain and

295 Gulf of Lion GSA (GSA 4); Ligurian Sea and Northern Tyrrhenian Sea and Southern and

296 Central Tyrrhenian Sea, creating the Tyrrhenian Sea GSA (GSA 6); Western and Eastern

297 Sardinia, creating the Sardinia GSA (GSA 7); Northern Tunisia, Gulf of Hammamet, and Gulf

298 of Gabès, creating the Tunisia GSA (GSA 8); Southern Sicily and Malta GSA (GSA 9); Northern

299 and Southern Adriatic Sea, creating the Adriatic Sea GSA (GSA 10); Crete and Aegean Sea,

300 creating the Aegean Sea GSA (GSA 14); Northern Levant Sea and Cyprus, creating the

301 Northern Levant Sea and Cyprus GSA (GSA 15); Southern and Eastern Levant Sea GSA (GSA

302 16). In addition, the Corsica GSA was not considered because it was included in the Pelagos

303 Sanctuary, while the Gulf of Lion and Ligurian Sea and Northern Tyrrhenian Sea were

304 reduced to avoid overlap with the Pelagos Sanctuary.

305 The ratio values in the Pelagos Sanctuary and in the GSAs were compared using a paired

306 sample Wilcoxon test with corrections applied for multiple testing; (ii) in the Mediterranean

307 areas where the total biomass of small pelagic fish is large according to simulations provided

308 by the end-to-end ecosystem model OSMOSE-MED (Moullec et al., 2019b). Results for the

309 other size classes are available in the Supplementary Material.

310

311 **2.5. The end-to-end model OSMOSE-MED**

312

313 OSMOSE-MED is an end-to-end modelling chain, including a general circulation model, a

314 regional climate model, a regional biogeochemistry model and a multispecies dynamic

315 model (OSMOSE; Moullec et al., 2019). OSMOSE is a spatially explicit individual-based model

316 which simulates the whole life cycle of several interacting fish and macro-invertebrates

317 species from eggs to adult stages. Major ecological processes of the life cycle, such as

318 growth, predation, reproduction, and mortality sources, are modelled step by step (15 days

319 in this study) (www.osmose-model.org; (Shin et al., 2004; Shin and Cury, 2001). OSMOSE-

320 MED covers the whole Mediterranean Sea and represents the Mediterranean food web

321 from pankton to main top-predators in the 2006-2013 period. Hundred marine species (fish,

322 cephalopods and crustaceans), representing ca. 95% of total declared catches in the region

323 over the 2006-2013 period were explicitly modelled. For a full description of the

324 parameterization and calibration of OSMOSE-MED (see Moullec et al., 2022, 2019a, 2019b).

325 The biomass of small pelagic fish is an output of OSMOSE-MED simulations. As OSMOSE is a

326 stochastic model, ten replicated simulations were run and averaged to analyse the outputs.

327 For this study, the total biomass of 10 small pelagic species only (e.g., European anchovy,

328 European sardine, Round sardinella or European sprat) was considered. Areas of small-

329 pelagic high biomass were defined as the locations with a biomass value higher than the

330 90th percentile of all the Mediterranean Sea biomass values. Results corresponding to the

331 80th and 95th percentiles are reported in the Supplementary Materials.

332

333   **III.**   **<u>Results</u>**

334 **3.1. Plastic and zooplankton distributions in the Mediterranean Sea and their drivers**

335 The predictive performance of the Xgboost model was assessed by calculating the

336 correlation coefficient (R^2) between observed and predicted values of plastic and

337 zooplankton abundance (Table 1, S4, S5, Figure S2, S3). R^2 coefficients were 0.68 and 0.57

for plastic debris and zooplankton abundances, respectively (Table 1). Overall, the

relationships found tended to overestimate low values and to underestimate large ones

(Figure S2, S3). R^2 is known to be sensitive to the extent of dependent variables (Gelman

and Hill, 2006) which range between 2260 N/km² and 7974561 N/km² in this study. This

could explain the low cross-validated R^2 which is strengthened by the low amount of

available data (122 sampling stations). High zooplankton abundances were associated with

negative Okubo-Weiss values (19 % of the explanatory power in the model, Fig. 2c), and

with positive and negative vorticity values (14%). Both these explanatory variables indicate

an eddy presence, and do not reveal a clear preference for cyclones or anticyclones. The

temperature influenced the total zooplankton abundance as well (16%), with lower

abundances associated with higher temperatures. Attracting fronts, identified by Finite-

Time Lyapunov Exponents (FTLEs, 9%) calculated backward in time, were positively

correlated with zooplankton abundance, while the relationship was of opposite sign with

diverging fronts (FTLE forward in time: 8%; and divergence: 7%). Explanatory variables that

most contributed to explain plastic debris abundance were the kinetic energy (50%) and TKE

(10%) (Figure 2d), indicating a greater concentration of plastic debris in retentive and low

turbulence regions. Nitrates (11%, a proxy for riverine outputs) indicated a positive

relationship between plastic debris presence and the proximity to river mouths.

When considering the plastic and zooplankton abundances projected over the entire

Mediterranean Sea (Fig. 2a,b), highest concentrations were mainly observed in the Adriatic

and Aegean Seas (GSAs 10 and 14 in Fig. 1, respectively). In these regions, abundances were

estimated around 20×10^6 N/km² for zooplankton (Figure 2a) and 5×10^6 N/km² for plastic

debris (Figure 2b). The Eastern basin (GSAs 15 and 16) presented low abundances of

361 zooplankton and plastic debris. However, the latter was abundant along Cyprus (located in

362 GSA 15) and Lebanon (located in GSA 16) coasts and in the Gulf of Gabès (located in GSA 8).

363 The Tyrrhenian Sea (GSA 6) was also a hotspot of plastic debris abundance. In the Strait of

364 Gibraltar (located in GSA 1), the models predicted high values of zooplankton abundances

365 and low plastic debris concentrations.

366 The results obtained with different size classes showed very similar patterns (Figure S4, S5

367 and S6), and high R^2 coefficients were obtained as well (Table S5). Plastic standard deviation

368 maps (Fig. S7a) show that the uncertainties corresponded to about 10% of the plastic

369 abundance values. The same considerations were valid for the zooplankton uncertainties

370 (Fig. S7b), showing the robustness of the models obtained.

371

372 **Table 1 :** Predictive performance and best parameters estimated by 4-fold cross validation for size

373 between 0.33 and 5 mm

	Predictive performance	Model parameters			
Group	R^2	trees	Maximum depth	Eta	Minimum child weight
Zooplankton (> 0.33 and < 5 mm)	0.57	707	2	0.04	5
Microplastic (> 0.33 and < 5 mm)	0.68	851	2	0.03	1

374

375
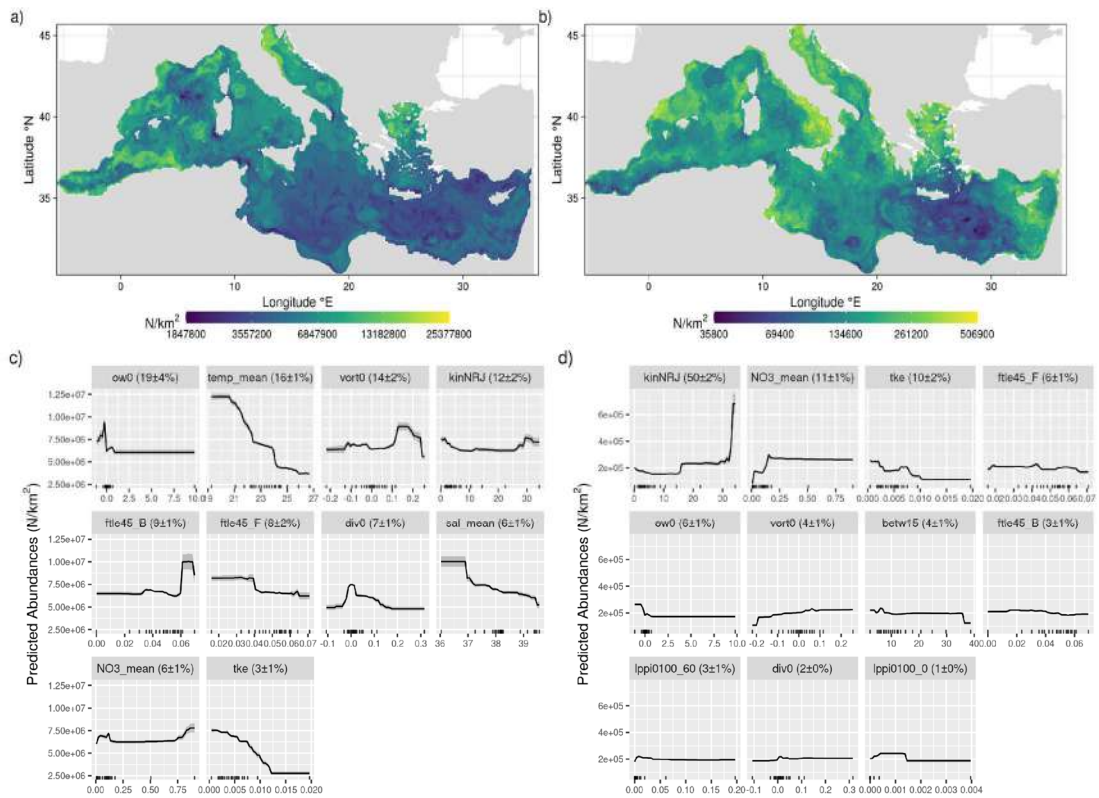
Figure 2 : Plastic and zooplankton abundances : Spatial projection and partial dependence plot of zooplankton (panels a and c, respectively) and plastic debris abundance (panels b and d, respectively) for the size class < 5 mm. oW0 = Okubo Weiss, kinNRJ = Kinetic Energy, temp_mean = mean temperature, NO3_mean = mean nitrate concentration, vort0 = vorticity , tke = Turbulent Kinetic Energy, ftle45_F = FTLE 45 days forward in time, ftle45_B = FTLE 45 days backward in time, div0 = Eulerian Divergence, betw15 = Betweenness at 15 days, sal_mean = mean salinity, lppi0100_60 = LPPI with distance threshold of 1° and 60 days backward in time, lppi0100_0 = LPPI with distance threshold of 1° and no advection

3.2. Plastic to zooplankton ratio

Using zooplankton and plastic debris abundance projections, we calculated the plastic to zooplankton ratio (number of plastic debris per km^2 divided by the number of zooplankton

18

387   organisms per km^2 , MM 2.4) over the entire Mediterranean Sea for the size class between

388   0.33—5 mm (Fig. 3a). The average plastic to zooplankton ratio was 0.029 (±0.012) at the

389   Mediterranean scale. Areas with the highest average plastic to zooplankton ratio were the

390   gulf of Gabès (located in GSA 8), the Cilician (GSA 15), the Levantine (GSA 15 and 16), and

391   the Southern Tyrrhenian Seas (GSA 6), with values of ~0.10. Intermediate values (~0.05)

392   were found in the Balearic (GSA 3) and Adriatic Seas (GSA 3) and in the Central

393   Mediterranean (GSA 13). Lower values (~ 0.01) were in the Alboran Sea (GSA 1) and the

394   central sector of the Eastern Mediterranean Sea (GSA 16 and eastern part of GSA 15).

395   When considering the results obtained with different size classes the spatial pattern did not

396   change consistently (Fig. S10). The ratio decreased to 0.004—0.1 when considering a size

397   class between 0.33—1 mm, while it increased to 0.005—0.3 when considering the size class

398   between 1 and 5 mm, due to the different abundances considered. The uncertainty on the

399   ratio (Fig. S7c) was greater in regions of larger ratio and lower elsewhere, and corresponded

400   to ~10% of the ratio value. These results show the soundness of this metric.
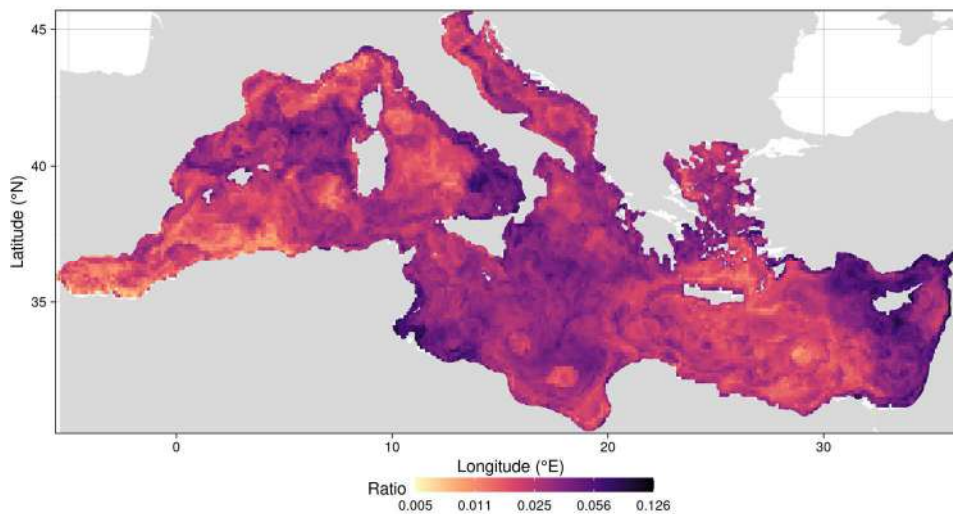
401

Figure 3 : Plastic to zooplankton ratio : Spatial projection of the plastic to zooplankton ratio

for the size class between 0.33—5 mm

3.3. Case studies

3.3.1. Wildlife exposure: plastic ingestion risk for small pelagic fish

The plastic to zooplankton ratio was applied to two case studies to analyse the probability of

plastic ingestion by wildlife as described in the next subsections.

In the first case study, we considered the total biomass of small pelagic fish in the

Mediterranean Sea for the time period 2006-2013, obtained from the Osmose model.

One of the largest Mediterranean hotspots of small pelagic fish, located in the Gulf of Gabès

(located in GSA 8), as well as a smaller one in the Cilician basin (between Cyprus and Turkey,

GSA 15), were found in correspondence with plastic to zooplankton ratios greater than 0.06

415   (Fig. 4a). Two large hotspots of small pelagic fish, in the Adriatic Sea (GSA 10) and in the

416   Southern Catalan Sea (GSA 4), were associated with moderate plastic to zooplankton ratios

417   greater than 0.03. The remaining part of the small pelagic hotspots was highly patchy and

418   mainly distributed along the coasts, with variable ratio values.

419   When using different percentiles to identify the main small pelagic fish hotspots (Fig. S9),

420   these were still located in the Adriatic Sea and in the Gulf of Gabès, confirming that these

421   hotspots were threatened by plastic pollution and providing evidence of the robustness of

422   the analyses.

423

424   **3.3.2   Wildlife exposure: plastic ingestion risk in the Pelagos Sanctuary and different**

425   **Mediterranean regions**

426

427   In the second case study, we calculated the plastic to zooplankton ratio in the Pelagos

428   Sanctuary and compared it with the ratio of 15 Mediterranean Sea GSAs (Fig.1). The Pelagos

429   Sanctuary showed ratio values which were significantly larger than those predicted in the

430   Alboran Sea (GSA 1), Algeria (GSA 2), Balearic Islands (GSA 3), Northern Spain and Gulf of

431   Lion (GSA 4) and Aegean Sea (GSA 14), while they were significantly lower than those in the

432   Tyrrhenian Sea (GSA 6), Southern Sicily and Malta (GSA 9), and the Northern Levant Sea

433   (GSA 16). No significant differences were found with other GSAs (Fig. 4b).

434

435

436
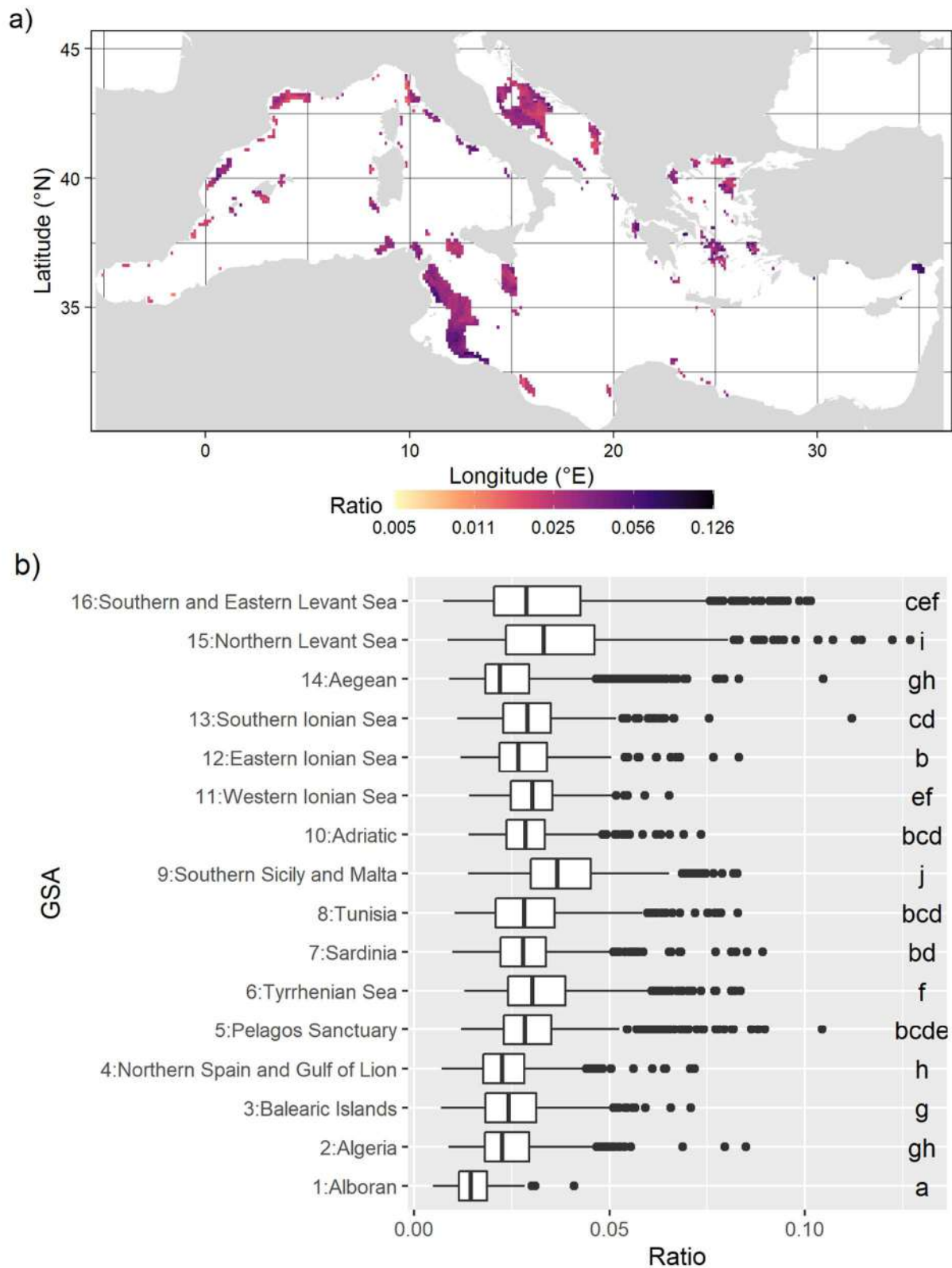
Figure 4 : Application of plastic to zooplankton ratio to two case studies : a) Plastic to

zooplankton ratio for plastic debris of size between 0.33—5 mm, showed only in

439 correspondence with the hotspots of small pelagic fish (defined as the locations with a

440 biomass larger than the 90th percentile), b) boxplot of ratio values in the Pelagos Sanctuary

441 and in 15 Mediterranean GSAs (shown in Fig. 1, MM 4). The letters on top of each box

442 display pairwise wilcoxon test results.

443

444   **IV.**   <u>**Discussion**</u>

445 **4.1. Zooplankton distribution in the Mediterranean Sea and its drivers**

446

447 Zooplankton abundance was boosted by eddy presence, even if no clear preference for

448 cyclones or anticyclones was detected. This was in accordance with previous studies finding

449 large zooplankton concentration in eddies (Chambault et al., 2019; Godø et al., 2012;

450 Riandey et al., 2005). Temperature played an important role in zooplankton abundances

451 which decreased when temperature increased. This is because temperature affects the

452 mixed layer depth (MLD) (D'Ortenzio et al., 2005). MLD governs the availability of nutrients

453 and light, which are essential for phytoplankton, the primary food source for zooplankton.

454 In regions with higher temperatures, such as the Levantine Basin, the MLD is relatively

455 shallow (due to a low mixing in winter and a strong stratification in summer): this hampers

456 nutrient supply to the phytoplankton, and in turn inhibits zooplankton growth; conversely,

457 in the western basin, colder, the MLD is deeper, boosting biological activity (D'Ortenzio et

458 al., 2005). High zooplankton abundance in coastal regions can also be attributed to

459 phytoplankton blooms occurring near highly populated coasts, subject to terrigenous and

460 river inputs in nutrients (Siokou-Frangou et al., 2010).

461 Frontal converging regions (identified through backward FTLE) were positively correlated

462   with zooplankton abundance. This is in coherence with previous studies highlighting the

463   importance of these features for mid trophic levels and, in general, the whole trophic chain

464   (Baudena et al., 2021; Chambault et al., 2017; d'Ovidio et al., 2010; Della Penna et al., 2015).

465   The negative correlation found with diverging zones (identified through forward FTLE and

466   divergence) suggest that these structures, even if fostering primary production, hamper

467   zooplankton concentration, possibly by spreading it away.

468   Notably, the pattern of zooplankton abundance over the whole Mediterranean was in

469   agreement with the average zooplankton mass in June–November 2014 obtained by the

470   Seapodym model (Lehodey et al., 2010; Fig. S11): the western Mediterranean showed larger

471   values than the eastern Mediterranean; the largest values were predicted in the northern

472   Adriatic Sea and in the Algerian and Alboran basins both by our projection and by the

473   Seapodym model. Differences could be explained by the fact that we used zooplankton

474   abundance (in N/km^2) while Seapodym provided zooplankton mass, and by the different

475   methodological approaches.

476

477   **4.2. Plastic debris distribution in the Mediterranean Sea and its drivers**

478

479   Plastic debris concentration obtained from the projections was lower in regions

480   characterised by strong currents and turbulence. This was confirmed by the decreasing

481   relationship found between plastic debris and kinetic energy (50 % of the variance), TKE,

482   and FTLE calculated both forward and backward in time (Fig. 2d). The positive relationship

483   found with nitrates, a proxy for land-based pollution (e.g. river mouths or cities), indicated

484   that plastic debris abundance was linked with coastal sources. This suggests that plastic

485   debris is released mainly from coastal sources, in coherence with previous studies (Baudena

486 et al., 2022; Liubartseva et al., 2018), where less energetic features are found. When plastic

487 debris moves offshore, turbulent activity and currents mix it, lowering plastic abundance.

488 This is corroborated by the slightly negative relationship with FTLE calculated both forward

489 and backward in time: plastic debris may be attracted by frontal converging regions but

490 then spread away.

491 The projection of plastic concentration does not show regions of strong plastic

492 accumulation. This is in coherence with previous studies (Baudena et al., 2022; Liubartseva

493 et al., 2018), which attributed this lack to the strong spatio-temporal variability of

494 Mediterranean currents.

495 The plastic concentration pattern we obtained was similar to the one reported by

496 (Liubartseva et al., 2018) despite the different methodological approach (a Lagrangian

497 tracking model). Higher concentrations of plastic debris were found in the northern Adriatic

498 and (GSA 10) in the Balearic and northern Spain Sea (GSAs 3 and 4) and in the Levantine

499 Basin (GSAs 15 and 16). Lower concentrations were found in the central part of the Eastern

500 Mediterranean (GSAs 14—16), in the Bomba Gulf (Southern part of GSA 13), and in the

501 Alboran Sea (GSA 1). A larger concentration was predicted in the Cilician basin (GSA 15) and

502 in a portion of the Gulf of Lion (GSA 4) by Liubartseva et al. (2018) model, likely driven by

503 the nearby presence of coastal plastic sources. This result provides evidence of the

504 soundness of the pattern we obtained.

505 Our model predicted a total of $4 \cdot 10^{11}$ plastic debris floating at the surface of the

506 Mediterranean Sea. This value was in agreement with the results from (Pedrotti et al.,

507 2022); $6 \cdot 10^{11}$, confidence interval $4—14 \cdot 10^{11}$). The difference may be explained by the fact

508 that our model predicted the plastic debris concentration over the entire basin and not only

509 at the location of the Tara Mediterranean Expedition stations.

510 In general, plastic models had better estimations than zooplankton models. This may be due

511 to the relatively easier description of plastic dynamics rather than zooplankton abundance,

512 which is driven by complex biological and ecological processes including growth, predation,

513 competition or behaviour including vertical migrations (Queré et al., 2005).

514

515 **4.3. Plastic to zooplankton ratio and wildlife exposure**

516

517 The plastic and zooplankton projections allowed us to calculate the plastic to zooplankton

518 ratio at the Mediterranean Sea scale. This ratio ranged approximately between 0.005 (i.e., 5

519 plastic debris every 1000 zooplankton organisms) and 0.100 (i.e., 100 plastic debris every

520 1000 zooplankton organisms) throughout the whole basin.

521 Our results on the risk of plastic ingestion for small pelagic fish suggested that they could

522 ingest large amounts of debris. Indeed, the ratio of plastic to zooplankton was moderate to

523 high in the two larger pelagic fish hotspots, located in the Gulf of Gabès (GSA 8) and in the

524 Adriatic Sea (GSA 10). This is of particular concern since both regions are heavily exploited

525 by fishing industries (Colloca et al., 2017). While we could not explicitly observe an ingestion

526 of plastic debris by small pelagic fish in situ, previous studies reported microplastic presence

527 in the stomach content of at least 87 fish species in the Mediterranean Sea (Habib et al.,

528 2021), many of them being commercially important (Jâms et al., 2020; Renzi et al., 2019).

529 The Pelagos Sanctuary showed plastic to zooplankton ratio values (0.031±0.014) significantly

530 larger than all the GSAs in the Western Mediterranean, with the exclusion of the Tyrrhenian

531 Sea, and which were comparable to several GSAs across the basin. This value was similar to

532 the average plastic to zooplankton ratio obtained in the northwestern Mediterranean by

533 Pedrotti et al., (2016) (2016; 0.03 ±1.40). These results highlight the potential ingestion of

534   plastic debris by whales in this region. Fossi et al., (2012) recorded phthalates (a main

535   constituent of plastic) in fin whale *Balaenoptera physalus* blubber, showing that they could

536   consume plastic debris directly or indirectly from water and plankton. Hence, these

537   mammals, among the largest filter feeders in the world and adapted to absorbing large

538   quantities of prey in a single mouthful, are threatened in one of their main feeding areas

539   which is heavily contaminated.

540   We stress that the latter cases are just two examples of how the plastic to zooplankton ratio

541   can be used to estimate the threat represented by plastic debris on marine biota and,

542   ultimately, on human health (Bhuyan et al., 2022). Several other applications are possible,

543   including the study of marine protected areas (Soto-Navarro et al., 2021), fishery grounds

544   (Colloca et al., 2017), or specific regional analyses, also unravelling the origin of the plastic

545   debris (Liubartseva et al., 2019).

546

547   **4.4. Limits**

548

549   The present study is not a mechanistic understanding of plastic debris ingestion by small

550   pelagic fish. Zooplankton communities and their quality as food supply for predators were

551   not assessed. Feuilloley et al. (2022), using a long time series of zooplankton observations in

552   the northwestern Mediterranean, showed that changes in zooplankton composition, size,

553   and density may impact higher trophic levels, such as the fitness of small pelagic fish.

554   Results should be considered cautiously as both plastic and zooplankton were averaged over

555   6 months in the same year (June—November 2014). We only analysed surface data, while

556   zooplankton organisms live in the whole water column and several species have a diel

557   vertical migration.

558 It was not possible to identify a value of plastic to zooplankton ratio over which the risk of

559 plastic ingestion could be considered high, as no studies have investigated this question to

560 date. A possible choice would be the percentile of the ratio distribution over the

561 Mediterranean Sea. However, as the plastic pollution is expected to increase in the future

562 (Borrelle et al., 2020; Lau et al., 2020), so will the ratio. Further studies are needed on this

563 issue.

564 Multiple caveats are associated with the use of statistical approaches in a dynamic

565 environment: i) they did not allow us to establish a causal relationship between

566 plastic/zooplankton abundances and environment; ii) they have limited capacities to

567 extrapolate in space and time (Guisan and Thuiller, 2005; Ralston and Moore, 2020; Yates et

568 al., 2018). However, these approaches have proved to be useful, valuable, and cost-effective

569 tools to quantify plastic/zooplankton distribution, especially in data-poor areas (Fabri-Ruiz

570 et al., 2019; Guillaumot et al., 2019).

571

572

573

574   **V.**   **Conclusions**

575

576 All in all, our findings showed that plastic debris is widespread in the Mediterranean Sea,

577 with a number of debris in a similar order of magnitude than zooplankton organisms across

578 the entire basin. This highlights the potential stress induced by this invasive element on the

579 marine ecosystems, and the necessity of further research efforts on these questions.

580 Further samplings of plastic debris and zooplankton organisms are needed, with larger

581 spatio-temporal resolutions and water column observations. In addition, the understanding

582 of the interaction between top predators, fish, and lower trophic levels in the presence of

583 plastic will be crucial to correctly assess the threat encountered and to design mitigation

584 strategies.

585

599

600 **Data availability**

601

602 All the data necessary to produce the figures of the Main Text, i.e. the plastic and

603 zooplankton abundances calculated over the whole Mediterranean Sea, the plastic to

604 zooplankton ratio, the partition of the different GSAs used, as well as the climatology of the

605   small pelagic fish biomass are available at https://doi.org/10.5281/zenodo.7076175. The in

606   situ plastic concentrations are available at https://doi.org/ 10.5281/zenodo.5538237. The

607   velocity field used to calculate the Lagrangian diagnostics are available on the E.U.

608   Copernicus Marine Environment Service Information website (CMEMS,

609   http://marine.copernicus.eu/).

610

611

612

613

614

615

616

617

618

619

620

621

622

623

624

625

626

627

628

629

630 **References**

631

632 Aretoulaki, E., Ponis, S., National Technical University Athens, Plakas, G., National

633   Technical University Athens, Agalianos, K., National Technical University Athens,

634   2021. Marine plastic littering: a review of socio economic impacts. J. Sustain. Sci.

635   Manag. 16, 276–300. https://doi.org/10.46754/jssm.2021.04.019

636 Babak, N., 2015. usdm: Uncertainty analysis for species distribution models. R package

637   version 1.1-15.

638 Baudena, A., Ser-Giacomi, E., D'Onofrio, D., Capet, X., Cotté, C., Cherel, Y., D'Ovidio, F.,

639   2021. Fine-scale structures as spots of increased fish concentration in the open

640   ocean. Sci. Rep. 11, 15805. https://doi.org/10.1038/s41598-021-94368-1

641 Baudena, A., Ser-Giacomi, E., Jalón-Rojas, I., Galgani, F., Pedrotti, M.L., 2022. The

642   streaming of plastic in the Mediterranean Sea. Nat. Commun. 13, 2981.

643   https://doi.org/10.1038/s41467-022-30572-5

644 Baudena, A., Ser-Giacomi, E., López, C., Hernández-García, E., d'Ovidio, F., 2019.

645   Crossroads of the mesoscale circulation. J. Mar. Syst. 192, 1–14.

646   https://doi.org/10.1016/j.jmarsys.2018.12.005

647 Beaumont, N.J., Aanesen, M., Austen, M.C., Börger, T., Clark, J.R., Cole, M., Hooper, T.,

648   Lindeque, P.K., Pascoe, C., Wyles, K.J., 2019. Global ecological, social and

649   economic impacts of marine plastic. Mar. Pollut. Bull. 142, 189–195.

650   https://doi.org/10.1016/j.marpolbul.2019.03.022

651 Bhuyan, Md.S., Rashed-Un-Nabi, Md., Alam, Md.W., Islam, Md.N., Cáceres-Farias, L., Bat,

652   L., Musthafa, M.S., Senapathi, V., Chung, S.Y., Núñez, A.A., 2022. Environmental

653   and Morphological Detrimental Effects of Microplastics on Marine Organisms to

654   Human Health (preprint). In Review. https://doi.org/10.21203/rs.3.rs-1290795/v1

655 Borrelle, S.B., Ringma, J., Law, K.L., Monnahan, C.C., Lebreton, L., McGivern, A., Murphy,

656   E., Jambeck, J., Leonard, G.H., Hilleary, M.A., Eriksen, M., Possingham, H.P., De

657   Frond, H., Gerber, L.R., Polidoro, B., Tahir, A., Bernard, M., Mallos, N., Barnes, M.,

658   Rochman, C.M., 2020. Predicted growth in plastic waste exceeds efforts to mitigate

659   plastic pollution. Science 369, 1515–1518. https://doi.org/10.1126/science.aba3656

660 Bray, L., Digka, N., Tsangaris, C., Camedda, A., Gambaiani, D., de Lucia, G.A., Matiddi, M.,

661   Miaud, C., Palazzo, L., Pérez-del-Olmo, A., Raga, J.A., Silvestri, C., Kaberi, H., 2019.

662   Determining suitable fish to monitor plastic ingestion trends in the Mediterranean

663   Sea. Environ. Pollut. 247, 1071–1077. https://doi.org/10.1016/j.envpol.2019.01.100

664 Chambault, P., Baudena, A., Bjorndal, K.A., Santos, M.A.R., Bolten, A.B., Vandeperre, F.,

665   2019. Swirling in the ocean: Immature loggerhead turtles seasonally target old

666   anticyclonic eddies at the fringe of the North Atlantic gyre. Prog. Oceanogr. 175,

667   345–358. https://doi.org/10.1016/j.pocean.2019.05.005

668 Chambault, P., Roquet, F., Benhamou, S., Baudena, A., Pauthenet, E., de Thoisy, B.,

669   Bonola, M., Dos Reis, V., Crasson, R., Brucker, M., Le Maho, Y., Chevallier, D.,

670   2017. The Gulf Stream frontal system: A key oceanographic feature in the habitat

671   selection of the leatherback turtle? Deep Sea Res. Part Oceanogr. Res. Pap. 123,

672   35–47. https://doi.org/10.1016/j.dsr.2017.03.003

673 Chen, T., Guestrin, C., 2016. XGBoost: A Scalable Tree Boosting System, in: Proceedings

674   of the 22nd ACM SIGKDD International Conference on Knowledge Discovery and

675   Data Mining. Presented at the KDD '16: The 22nd ACM SIGKDD International

676   Conference on Knowledge Discovery and Data Mining, ACM, San Francisco

677   California USA, pp. 785–794. https://doi.org/10.1145/2939672.2939785

678 Chen, T., He, T., Benesty, M., Khotilovich, V., Tang, Y., Cho, H., Chen, K., 2015. Xgboost:

679   extreme gradient boosting. R Package Version 04-2 1, 1–4.

680 Cole, M., Lindeque, P., Halsband, C., Galloway, T.S., 2011. Microplastics as contaminants in

681   the marine environment: A review. Mar. Pollut. Bull. 62, 2588–2597.

682   https://doi.org/10.1016/j.marpolbul.2011.09.025

683 Coll, M., Piroddi, C., Steenbeek, J., Kaschner, K., Ben Rais Lasram, F., Aguzzi, J.,

684   Ballesteros, E., Bianchi, C.N., Corbera, J., Dailianis, T., Danovaro, R., Estrada, M.,

685   Froglia, C., Galil, B.S., Gasol, J.M., Gertwagen, R., Gil, J., Guilhaumon, F., Kesner-

686   Reyes, K., Kitsos, M.-S., Koukouras, A., Lampadariou, N., Laxamana, E., López-Fé

687   de la Cuadra, C.M., Lotze, H.K., Martin, D., Mouillot, D., Oro, D., Raicevich, S., Rius-

688   Barile, J., Saiz-Salinas, J.I., San Vicente, C., Somot, S., Templado, J., Turon, X.,

689   Vafidis, D., Villanueva, R., Voultsiadou, E., 2010. The Biodiversity of the

690   Mediterranean Sea: Estimates, Patterns, and Threats. PLoS ONE 5, e11842.

691   https://doi.org/10.1371/journal.pone.0011842

692   Collignon, A., Hecq, J.-H., Galgani, F., Collard, F., Goffart, A., 2014. Annual variation in

693   neustonic micro- and meso-plastic particles and zooplankton in the Bay of Calvi

694   (Mediterranean–Corsica). Mar. Pollut. Bull. 79, 293–298.

695   https://doi.org/10.1016/j.marpolbul.2013.11.023

696   Colloca, F., Scarcella, G., Libralato, S., 2017. Recent Trends and Impacts of Fisheries

697   Exploitation on Mediterranean Stocks and Ecosystems. Front. Mar. Sci. 4, 244.

698   https://doi.org/10.3389/fmars.2017.00244

699   Cózar, A., Sanz-Martín, M., Martí, E., González-Gordillo, J.I., Ubeda, B., Gálvez, J.Á.,

700   Irigoien, X., Duarte, C.M., 2015. Plastic Accumulation in the Mediterranean Sea.

701   PLOS ONE 10, e0121762. https://doi.org/10.1371/journal.pone.0121762

702   Croll, D.A., Tershy, B.R., Newton, K.M., de Vos, A., Hazen, E., Goldbogen, J.A., 2018. Filter

703   feeding, in: Encyclopedia of Marine Mammals. Elsevier, pp. 363–368.

704   d'Ovidio, F., De Monte, S., Alvain, S., Dandonneau, Y., Lévy, M., 2010. Fluid dynamical

705   niches of phytoplankton types. Proc. Natl. Acad. Sci. 107, 18366–18370.

706   https://doi.org/10.1073/pnas.1004620107

707   d'Ovidio, F., Della Penna, A., Trull, T.W., Nencioli, F., Pujol, M.-I., Rio, M.-H., Park, Y.-H.,

708   Cotté, C., Zhou, M., Blain, S., 2015. The biogeochemical structuring role of horizontal

709   stirring: Lagrangian perspectives on iron delivery downstream of the Kerguelen

710   Plateau. Biogeosciences 12, 5567–5581. https://doi.org/10.5194/bg-12-5567-2015

711   d'Ovidio, F., Fernández, V., Hernández-García, E., López, C., 2004. Mixing structures in the

712   Mediterranean Sea from finite-size Lyapunov exponents: Mixing structures in the

713   Mediterranean sea. Geophys. Res. Lett. 31, n/a-n/a.

714   https://doi.org/10.1029/2004GL020328

715 Della Penna, A., De Monte, S., Kestenare, E., Guinet, C., d'Ovidio, F., 2015. Quasi-

716   planktonic behavior of foraging top marine predators. Sci. Rep. 5, 18063.

717   https://doi.org/10.1038/srep18063

718 Dormann, C.F., Elith, J., Bacher, S., Buchmann, C., Carl, G., Carré, G., Marquéz, J.R.G.,

719   Gruber, B., Lafourcade, B., Leitão, P.J., Münkemüller, T., McClean, C., Osborne,

720   P.E., Reineking, B., Schröder, B., Skidmore, A.K., Zurell, D., Lautenbach, S., 2013.

721   Collinearity: a review of methods to deal with it and a simulation study evaluating

722   their performance. Ecography 36, 27–46. https://doi.org/10.1111/j.1600-

723   0587.2012.07348.x

724 D'Ortenzio, F., Iudicone, D., de Boyer Montegut, C., Testor, P., Antoine, D., Marullo, S.,

725   Santoleri, R., Madec, G., 2005. Seasonal variability of the mixed layer depth in the

726   Mediterranean Sea as derived from in situ profiles: mixed layer depth over the

727   Mediterranean. Geophys. Res. Lett. 32, n/a-n/a.

728   https://doi.org/10.1029/2005GL022463

729 Doyle, M.J., Watson, W., Bowlin, N.M., Sheavly, S.B., 2011. Plastic particles in coastal

730   pelagic ecosystems of the North-East Pacific ocean. Mar. Environ. Res. 71, 41–52.

731   https://doi.org/10.1016/j.marenvres.2010.10.001

732 Fabri☐Ruiz, S., Danis, B., David, B., Saucède, T., 2019. Can we generate robust species

733   distribution models at the scale of the Southern Ocean? Divers. Distrib. 25, 21–37.

734   https://doi.org/10.1111/ddi.12835

735 Feuilloley, G., Fromentin, J.-M., Saraux, C., Irisson, J.-O., Jalabert, L., Stemmann, L., 2022.

736   Temporal fluctuations in zooplankton size, abundance, and taxonomic composition

737   since 1995 in the North Western Mediterranean Sea. ICES J. Mar. Sci. 79, 882–900.

738   https://doi.org/10.1093/icesjms/fsab190

739 Fitzpatrick, M.C., Lachmuth, S., Haydt, N.T., 2021. The ODMAP protocol: a new tool for

740   standardized reporting that could revolutionize species distribution modeling.

741   Ecography 44, 1067–1070. https://doi.org/10.1111/ecog.05700

742 Fossi, M.C., Coppola, D., Baini, M., Giannetti, M., Guerranti, C., Marsili, L., Panti, C., de

743   Sabata, E., Clò, S., 2014. Large filter feeding marine organisms as indicators of

744   microplastic in the pelagic environment: The case studies of the Mediterranean

745   basking shark (*Cetorhinus maximus*) and fin whale (*Balaenoptera physalus*). Mar.

746   Environ. Res. 100, 17–24. https://doi.org/10.1016/j.marenvres.2014.02.002

747 Fossi, M.C., Panti, C., Guerranti, C., Coppola, D., Giannetti, M., Marsili, L., Minutoli, R.,

748   2012. Are baleen whales exposed to the threat of microplastics? A case study of the

749   Mediterranean fin whale (*Balaenoptera physalus*). Mar. Pollut. Bull. 64, 2374–2379.

750   https://doi.org/10.1016/j.marpolbul.2012.08.013

751 Friedman, J.H., 2001. Greedy function approximation: a gradient boosting machine. Ann.

752   Stat. 1189–1232.

753 Galgani, F., Claro, F., Depledge, M., Fossi, C., 2014. Monitoring the impact of litter in large

754   vertebrates in the Mediterranean Sea within the European Marine Strategy

755   Framework Directive (MSFD): Constraints, specificities and recommendations. Mar.

756   Environ. Res. 100, 3–9. https://doi.org/10.1016/j.marenvres.2014.02.003

757 Garrido, S., Ben-Hamadou, R., Oliveira, P., Cunha, M., Chícharo, M., van der Lingen, C.,

758   2008. Diet and feeding intensity of sardine *Sardina pilchardus*: correlation with

759   satellite-derived chlorophyll data. Mar. Ecol. Prog. Ser. 354, 245–256.

760   https://doi.org/10.3354/meps07201

761 Garrido, S., Marçalo, A., Zwolinski, J., van der Lingen, C., 2007. Laboratory investigations on

762   the effect of prey size and concentration on the feeding behaviour of *Sardina*

763   *pilchardus*. Mar. Ecol. Prog. Ser. 330, 189–199. https://doi.org/10.3354/meps330189

764 Gelman, A., Hill, J., 2006. Data Analysis Using Regression and Multilevel/Hierarchical

765   Models. Cambridge University Press.

766 Gerigny, O., Brun, M., Fabri, M.C., Tomasino, C., Le Moigne, M., Jadaud, A., Galgani, F.,

767   2019. Seafloor litter from the continental shelf and canyons in French Mediterranean

768   Water: Distribution, typologies and trends. Mar. Pollut. Bull. 146, 653–666.

769   https://doi.org/10.1016/j.marpolbul.2019.07.030

770   Gérigny, O., Pedrotti, M.-L., El Rakwe, M., Brun, M., Pavec, M., Henry, M., Mazeas, F.,

771   Maury, J., Garreau, P., Galgani, F., 2022. Characterization of floating microplastic

772   contamination in the bay of Marseille (French Mediterranean Sea) and its impact on

773   zooplankton and mussels. Mar. Pollut. Bull. 175, 113353.

774   https://doi.org/10.1016/j.marpolbul.2022.113353

775   Godø, O.R., Samuelsen, A., Macaulay, G.J., Patel, R., Hjøllo, S.S., Horne, J., Kaartvedt, S.,

776   Johannessen, J.A., 2012. Mesoscale Eddies Are Oases for Higher Trophic Marine

777   Life. PLoS ONE 7, e30161. https://doi.org/10.1371/journal.pone.0030161

778   Gorsky, G., Ohman, M.D., Picheral, M., Gasparini, S., Stemmann, L., Romagnan, J.-B.,

779   Cawood, A., Pesant, S., Garcia-Comas, C., Prejger, F., 2010. Digital zooplankton

780   image analysis using the ZooScan integrated system. J. Plankton Res. 32, 285–303.

781   https://doi.org/10.1093/plankt/fbp124

782   Gove, J.M., Whitney, J.L., McManus, M.A., Lecky, J., Carvalho, F.C., Lynch, J.M., Li, J.,

783   Neubauer, P., Smith, K.A., Phipps, J.E., Kobayashi, D.R., Balagso, K.B., Contreras,

784   E.A., Manuel, M.E., Merrifield, M.A., Polovina, J.J., Asner, G.P., Maynard, J.A.,

785   Williams, G.J., 2019. Prey-size plastics are invading larval fish nurseries. Proc. Natl.

786   Acad. Sci. 116, 24143–24149. https://doi.org/10.1073/pnas.1907496116

787   Guillaumot, C., Artois, J., Saucède, T., Demoustier, L., Moreau, C., Eléaume, M., Agüera, A.,

788   Danis, B., 2019. Broad-scale species distribution models applied to data-poor areas.

789   Prog. Oceanogr. 175, 198–207. https://doi.org/10.1016/j.pocean.2019.04.007

790   Guisan, A., Thuiller, W., 2005. Predicting species distribution: offering more than simple

791   habitat models. Ecol. Lett. 8, 993–1009. https://doi.org/10.1111/j.1461-

792   0248.2005.00792.x

793   Hernández-Carrasco, I., Orfila, A., Rossi, V., Garçon, V., 2018. Effect of small scale

794   transport processes on phytoplankton distribution in coastal seas. Sci. Rep. 8, 8613.

795   https://doi.org/10.1038/s41598-018-26857-9

796   Jâms, I.B., Windsor, F.M., Poudevigne-Durance, T., Ormerod, S.J., Durance, I., 2020.

797   Estimating the size distribution of plastics ingested by animals. Nat. Commun. 11,

798   1594. https://doi.org/10.1038/s41467-020-15406-6

799 Kershaw, P.J., Turra, A., Galgani, F., 2019. Guidelines for the monitoring and assessment of

800   plastic litter and microplastics in the ocean.

801 Lattin, G.L., Moore, C.J., Zellers, A.F., Moore, S.L., Weisberg, S.B., 2004. A comparison of

802   neustonic plastic and zooplankton at different depths near the southern California

803   shore. Mar. Pollut. Bull. 49, 291–294. https://doi.org/10.1016/j.marpolbul.2004.01.020

804 Lau, W.W.Y., Shiran, Y., Bailey, R.M., Cook, E., Stuchtey, M.R., Koskella, J., Velis, C.A.,

805   Godfrey, L., Boucher, J., Murphy, M.B., Thompson, R.C., Jankowska, E., Castillo

806   Castillo, A., Pilditch, T.D., Dixon, B., Koerselman, L., Kosior, E., Favoino, E.,

807   Gutberlet, J., Baulch, S., Atreya, M.E., Fischer, D., He, K.K., Petit, M.M., Sumaila,

808   U.R., Neil, E., Bernhofen, M.V., Lawrence, K., Palardy, J.E., 2020. Evaluating

809   scenarios toward zero plastic pollution. Science 369, 1455–1461.

810   https://doi.org/10.1126/science.aba9475

811 Le Bourg, B., Bănaru, D., Saraux, C., Nowaczyk, A., Le Luherne, E., Jadaud, A., Bigot, J.L.,

812   Richard, P., 2015. Trophic niche overlap of sprat and commercial small pelagic

813   teleosts in the Gulf of Lions (NW Mediterranean Sea). J. Sea Res. 103, 138–146.

814   https://doi.org/10.1016/j.seares.2015.06.011

815 Lefebvre, C., Saraux, C., Heitz, O., Nowaczyk, A., Bonnet, D., 2019. Microplastics FTIR

816   characterisation and distribution in the water column and digestive tracts of small

817   pelagic fish in the Gulf of Lions. Mar. Pollut. Bull. 142, 510–519.

818   https://doi.org/10.1016/j.marpolbul.2019.03.025

819 Liubartseva, S., Coppini, G., Lecci, R., 2019. Are Mediterranean Marine Protected Areas

820   sheltered from plastic pollution? Mar. Pollut. Bull. 140, 579–587.

821   https://doi.org/10.1016/j.marpolbul.2019.01.022

822 Liubartseva, S., Coppini, G., Lecci, R., Clementi, E., 2018. Tracking plastics in the

823   Mediterranean: 2D Lagrangian model. Mar. Pollut. Bull. 129, 151–162.

824   https://doi.org/10.1016/j.marpolbul.2018.02.019

825   Mansui, J., Darmon, G., Ballerini, T., van Canneyt, O., Ourmieres, Y., Miaud, C., 2020.

826   Predicting marine litter accumulation patterns in the Mediterranean basin: Spatio-

827   temporal variability and comparison with empirical data. Prog. Oceanogr. 182,

828   102268. https://doi.org/10.1016/j.pocean.2020.102268

829   Moore, C.J., Moore, S.L., Weisberg, S.B., Lattin, G.L., Zellers, A.F., 2002. A comparison of

830   neustonic plastic and zooplankton abundance in southern California's coastal waters.

831   Mar. Pollut. Bull. 44, 1035–1038. https://doi.org/10.1016/S0025-326X(02)00150-9

832   Morgado, C., Martins, A., Rosso, M., Moulins, A., Tepsich, P., 2017. Fin Whale Presence

833   and Distribution in the Pelagos Sanctuary: Temporal and Spatial Variability Along 2

834   Fixed-Line Transects Monitored in 2009-2013 14.

835   Moullec, F., Barrier, N., Drira, S., Guilhaumon, F., Hattab, T., Peck, M.A., Shin, Y.-J., 2022.

836   Using species distribution models only may underestimate climate change impacts

837   on future marine biodiversity. Ecol. Model. 464, 109826.

838   https://doi.org/10.1016/j.ecolmodel.2021.109826

839   Moullec, F., Barrier, N., Drira, S., Guilhaumon, F., Marsaleix, P., Somot, S., Ulses, C., Velez,

840   L., Shin, Y.-J., 2019a. An End-to-End Model Reveals Losers and Winners in a

841   Warming Mediterranean Sea. Front. Mar. Sci. 6, 345.

842   https://doi.org/10.3389/fmars.2019.00345

843   Moullec, F., Velez, L., Verley, P., Barrier, N., Ulses, C., Carbonara, P., Esteban, A., Follesa,

844   C., Gristina, M., Jadaud, A., Ligas, A., Díaz, E.L., Maiorano, P., Peristeraki, P.,

845   Spedicato, M.T., Thasitis, I., Valls, M., Guilhaumon, F., Shin, Y.-J., 2019b. Capturing

846   the big picture of Mediterranean marine biodiversity with an end-to-end model of

847   climate and fishing impacts. Prog. Oceanogr. 178, 102179.

848   https://doi.org/10.1016/j.pocean.2019.102179

849   Onink, V., Wichmann, D., Delandmeter, P., Sebille, E., 2019. The Role of Ekman Currents,

850   Geostrophy, and Stokes Drift in the Accumulation of Floating Microplastic. J.

851   Geophys. Res. Oceans 124, 1474–1490. https://doi.org/10.1029/2018JC014547

852   Pedrotti, M.L., Lombard, F., Baudena, A., Galgani, F., Elineau, A., Petit, S., Henry, M.,

853   Troublé, R., Reverdin, G., Ser-Giacomi, E., Kedzierski, M., Boss, E., Gorsky, G.,

854   2022. An integrative assessment of the plastic debris load in the Mediterranean Sea.

855   Sci. Total Environ. 838, 155958. https://doi.org/10.1016/j.scitotenv.2022.155958

856   Pedrotti, M.L., Petit, S., Elineau, A., Bruzaud, S., Crebassa, J.-C., Dumontet, B., Martí, E.,

857   Gorsky, G., Cózar, A., 2016. Changes in the Floating Plastic Pollution of the

858   Mediterranean Sea in Relation to the Distance to Land. PLOS ONE 11, e0161581.

859   https://doi.org/10.1371/journal.pone.0161581

860   Pennino, M.G., Bachiller, E., Lloret-Lloret, E., Albo-Puigserver, M., Esteban, A., Jadaud, A.,

861   Bellido, J.M., Coll, M., 2020. Ingestion of microplastics and occurrence of parasite

862   association in Mediterranean anchovy and sardine. Mar. Pollut. Bull. 158, 111399.

863   https://doi.org/10.1016/j.marpolbul.2020.111399

864   Picheral, M., Colin, S., Irisson, J.O., 2017. EcoTaxa, a tool for the taxonomic classification of

865   images. URL Httpecotaxa Obs-Vlfr Fr.

866   Provencher, J.F., Ammendolia, J., Rochman, C.M., Mallory, M.L., 2019. Assessing plastic

867   debris in aquatic food webs: what we know and don't know about uptake and trophic

868   transfer. Environ. Rev. 27, 304–317. https://doi.org/10.1139/er-2018-0079

869   Queiros, Q., Fromentin, J.-M., Gasset, E., Dutto, G., Huiban, C., Metral, L., Leclerc, L.,

870   Schull, Q., McKenzie, D.J., Saraux, C., 2019. Food in the Sea: Size Also Matters for

871   Pelagic Fish. Front. Mar. Sci. 6, 385. https://doi.org/10.3389/fmars.2019.00385

872   Ralston, D.K., Moore, S.K., 2020. Modeling harmful algal blooms in a changing climate.

873   Harmful Algae 91, 101729. https://doi.org/10.1016/j.hal.2019.101729

874   Renzi, M., Specchiulli, A., Blašković, A., Manzo, C., Mancinelli, G., Cilenti, L., 2019. Marine

875   litter in stomach content of small pelagic fishes from the Adriatic Sea: sardines

876   (*Sardina pilchardus*) and anchovies (*Engraulis encrasicolus*). Environ. Sci. Pollut.

877   Res. 26, 2771–2781. https://doi.org/10.1007/s11356-018-3762-8

878   Riandey, V., Champalbert, G., Carlotti, F., Taupier-Letage, I., Thibault-Botha, D., 2005.

879   Zooplankton distribution related to the hydrodynamic features in the Algerian Basin

880   (western Mediterranean Sea) in summer 1997. Deep Sea Res. Part Oceanogr. Res.

881   Pap. 52, 2029–2048. https://doi.org/10.1016/j.dsr.2005.06.004

882 Rochman, C.M., Tahir, A., Williams, S.L., Baxa, D.V., Lam, R., Miller, J.T., Teh, F.-C.,

883   Werorilangi, S., Teh, S.J., 2015. Anthropogenic debris in seafood: Plastic debris and

884   fibers from textiles in fish and bivalves sold for human consumption. Sci. Rep. 5,

885   14340. https://doi.org/10.1038/srep14340

886 Savoca, M.S., McInturf, A.G., Hazen, E.L., 2021. Plastic ingestion by marine fish is

887   widespread and increasing. Glob. Change Biol. 27, 2188–2199.

888   https://doi.org/10.1111/gcb.15533

889 Ser-Giacomi, E., Baudena, A., Rossi, V., Follows, M., Clayton, S., Vasile, R., López, C.,

890   Hernández-García, E., 2021. Lagrangian betweenness as a measure of bottlenecks

891   in dynamical systems with oceanographic examples. Nat. Commun. 12, 4935.

892   https://doi.org/10.1038/s41467-021-25155-9

893 Shin, Y.-J., Cury, P., 2001. Exploring fish community dynamics through size-dependent

894   trophic interactions using a spatialized individual-based model. Aquat Living Resour

895   16. https://doi.org/10.1016/S0990-7440(01)01106-8

896 Shin, Y.-J., Shannon, L.J., Cury, P.M., 2004. Simulations of fishing effects on the southern

897   Benguela fish community using an individual-based model: learning from a

898   comparison with ECOSIM. Afr. J. Mar. Sci. 26, 95–114.

899   https://doi.org/10.2989/18142320409504052

900 Simoncelli, S., Fratianni, C., Pinardi, N., Grandi, A., Drudi, M., Oddo, P., Dobricic, S., 2014.

901   Mediterranean Sea physical reanalysis (MEDREA 1987–2015)(Version 1). Copernic

902   Monit Env. Mar Serv CMEMS 10.

903 Siokou-Frangou, I., Christaki, U., Mazzocchi, M.G., Montresor, M., Ribera d'Alcalá, M.,

904   Vaqué, D., Zingone, A., 2010. Plankton in the open Mediterranean Sea: a review.

905   Biogeosciences 7, 1543–1586. https://doi.org/10.5194/bg-7-1543-2010

906 Solomando, A., Pujol, F., Sureda, A., Pinya, S., 2022. Ingestion and characterization of

907   plastic debris by loggerhead sea turtle, *Caretta caretta*, in the Balearic Islands. Sci.

908   Total Environ. 826, 154159. https://doi.org/10.1016/j.scitotenv.2022.154159

909   Soto-Navarro, J., Jordá, G., Compa, M., Alomar, C., Fossi, M.C., Deudero, S., 2021. Impact

910   of the marine litter pollution on the Mediterranean biodiversity: A risk assessment

911   study with focus on the marine protected areas. Mar. Pollut. Bull. 165, 112169.

912   https://doi.org/10.1016/j.marpolbul.2021.112169

913   Wei, T., Simko, V., Levy, M., Xie, Y., Jin, Y., Zemla, J., 2017. Package 'corrplot.' Statistician

914   56, e24.

915   Yates, K.L., Bouchet, P.J., Caley, M.J., Mengersen, K., Randin, C.F., Parnell, S., Fielding,

916   A.H., Bamford, A.J., Ban, S., Barbosa, A.M., Dormann, C.F., Elith, J., Embling, C.B.,

917   Ervin, G.N., Fisher, R., Gould, S., Graf, R.F., Gregr, E.J., Halpin, P.N., Heikkinen,

918   R.K., Heinänen, S., Jones, A.R., Krishnakumar, P.K., Lauria, V., Lozano-Montes, H.,

919   Mannocci, L., Mellin, C., Mesgaran, M.B., Moreno-Amat, E., Mormede, S., Novaczek,

920   E., Oppel, S., Ortuño Crespo, G., Peterson, A.T., Rapacciuolo, G., Roberts, J.J.,

921   Ross, R.E., Scales, K.L., Schoeman, D., Snelgrove, P., Sundblad, G., Thuiller, W.,

922   Torres, L.G., Verbruggen, H., Wang, L., Wenger, S., Whittingham, M.J., Zharikov, Y.,

923   Zurell, D., Sequeira, A.M.M., 2018. Outstanding Challenges in the Transferability of

924   Ecological Models. Trends Ecol. Evol. 33, 790–802.

925   https://doi.org/10.1016/j.tree.2018.08.001

926   Zurell, D., Franklin, J., König, C., Bouchet, P.J., Dormann, C.F., Elith, J., Fandos, G., Feng,

927   X., Guillera-Arroita, G., Guisan, A., Lahoz-Monfort, J.J., Leitão, P.J., Park, D.S.,

928   Peterson, A.T., Rapacciuolo, G., Schmatz, D.R., Schröder, B., Serra-Diaz, J.M.,

929   Thuiller, W., Yates, K.L., Zimmermann, N.E., Merow, C., 2020. A standard protocol

930   for reporting species distribution models. Ecography 43, 1261–1277.

931   https://doi.org/10.1111/ecog.04960

932